Mathematical model of the human respiratory system in chronic obstructive pulmonary disease

Fleur T. Tehrani ✉

Department of Electrical Engineering, California State University, Fullerton, California 92831, USA
✉ *E-mail: ftehrani@fullerton.edu*

Published in Healthcare Technology Letters; Received on 29th July 2020; Revised on 12th October 2020; Accepted on 30th October 2020

Chronic obstructive pulmonary disease (COPD) is a respiratory illness with high rates of morbidity and mortality. The human respiratory system undergoes many chronic changes and adaptations under this disease conditions. The purpose of this study was to devise a mathematical model of the human respiratory system under COPD. The model presented is based on a previous detailed model of the human respiratory system. Cyclic changes of the lung volume with the effects of increased dead space are included and the lung mechanics are used to adjust the rate of breathing. Continuous and dynamic changes in the cardiac output and cerebral blood flow are represented in the model. The model includes the modified response of the respiratory control system under the chronic effects of COPD including the shifting of the acid–base balance under the disease conditions. The performance of the model has been examined at rest and during moderate exercise with and without oxygen supplementation. The results under different stimuli are found to be in general agreement with experimental observations.

1. Introduction: Chronic obstructive pulmonary disease (COPD) is a progressive respiratory illness which causes ventilator dependence [1, 2], disability [3, 4] and large numbers of death per year worldwide. In COPD, alveoli get damaged over time affecting the gas exchange in the lungs [5, 6] and reducing the ventilation/perfusion ratio [7]. In addition, the lung bronchi get inflamed leading to increase in the respiratory airway resistance and the work of breathing which in turn cause persistent cough and mucus production. These conditions lead to chronic hypoxemia and hypercapnia that in turn cause acid–base shift in the blood and the cerebrospinal fluid (CSF) [1, 2], alter the response of the respiratory control system to various stimuli and affect the functions of all the body organs as the disease progresses over time.

The study of the human respiratory system is not new and many models have been presented to represent the system mathematically and used in practice to study the features of the system. Works in [8–13] are a small selection of the models and simulation studies that have been previously published on this subject. A number of mathematical models representing multiple lung compartments with various ventilation/perfusion ratios have been presented with applications in COPD (e.g. [14, 15]). However, the previous models do not include the chronic adaptations of the respiratory control system in COPD and do not realistically represent the system under this disease conditions. The purpose of this study was to develop a mathematical model to represent the human respiratory system in COPD. A previous detailed model of the respiratory system [9] was used and modified to reflect the system's chronic adaptations. The ventilation control mechanisms were modified and new mathematical formulas for control of ventilation were devised. New and modified formulas for control of cardiac output and cerebral blood flow were also derived and used in the model. The model was tested at two stages of COPD, at rest, and in moderate exercise, with and without oxygen supplementation. The dynamic and steady-state results were compared with the reported experimental data in the literature.

2. Methods: The general structure of the mathematical model is shown in the block diagram of Fig. 1. As seen in this figure, the model is divided to a plant and a controller. The controller is designed to update and generate a respiratory drive signal for every breath. The controller consists of a 'mean value detector' that receives the information about the chemical composition of the arterial blood [16] and the blood at the neighbourhood of the central respiratory receptors [17, 18] and determines the average data over each breathing cycle. This information along with data indicative of the metabolic rate from the plant is used by a 'ventilation controller' to determine the required ventilation. A 'rate optimiser' receives the required ventilation data and determines the optimal respiration rate for a next breath based on the mechanical properties of the respiratory system to minimise the respiratory work rate [19]. A cyclic drive signal is then generated and sent to the lungs, which is updated for every breath.

The plant in Fig. 1 includes subsystems 'lungs', 'body tissue', 'brain tissue', a 'cerebrospinal fluid' compartment, a 'transport delay', that simulates the delay in arterial transport from the heart to the brain, 'peripheral receptors', 'central receptors' and a 'metabolic unit', that produces a neurogenic metabolic drive signal to activate the respiratory control system. The plant further includes a 'cardiac output controller', and a 'cerebral blood flow controller', that dynamically respond to the subject's bodily requirements by adjusting the cardiac output and the cerebral blood flow, respectively.

The mathematical descriptions and the equations of the respiratory controller, the modified equations for the 'cardiac output controller' and the 'cerebral blood flow controller', that are devised particularly for this model are derived and described in the following sections. The blocks and the equations of the model that are the same as those in [9] are provided in Appendix 1 and a list of the symbols and variables is provided in Appendix 2.

2.1. Respiratory control under COPD: COPD is a chronic and progressive respiratory illness that causes hypoxemia and hypercapnia as the disease advances. To compensate for these conditions, the human respiratory control system undergoes changes and adaptations over time. In COPD patients, there is a shift in the acid–base balance [1], reduction of the ventilation/perfusion ratio [5], increases in the dead space volume and respiratory airway resistance [6] and increases in the work of breathing affecting the breathing rate and pattern. The following section describes the derivation of formulas for the respiratory controller under COPD.

2.2. Ventilation controller: It was proposed several decades ago that the ventilatory response of the human respiratory control system is a

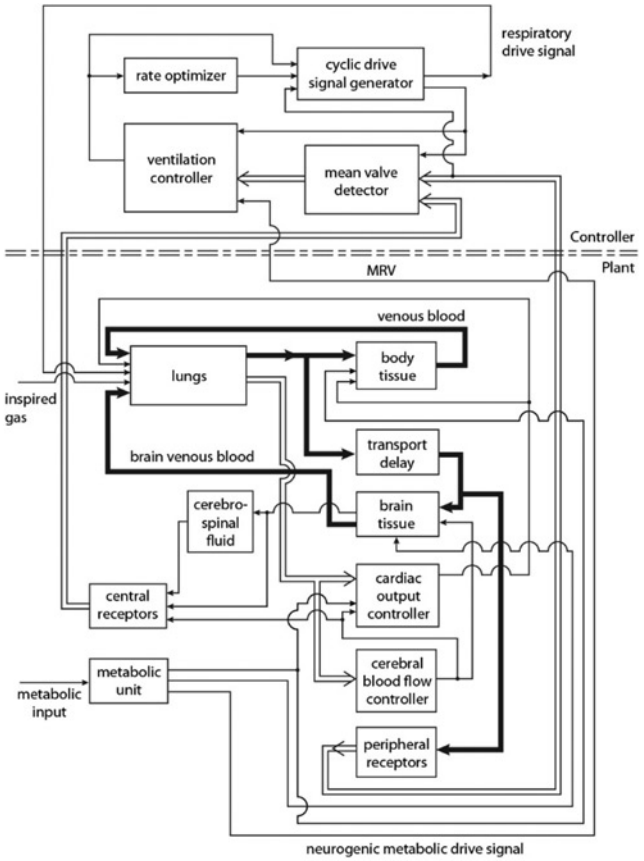

Fig. 1 *Model block diagram – CO_2 (thick black line), O_2 main blood circulation*

function of hydrogen ion concentration of the blood (H^+), the partial pressure of carbon dioxide in the arterial blood and the partial pressure of oxygen in the arterial blood [20]. On the basis of that theory, an equation for ventilation can be derived for normal subjects as [9]

$$\mathrm{AVR} = 0.22 \cdot H^+ + 0.262 \cdot P'_{a\mathrm{CO2(mean)}} + \mathrm{FACTV}\text{-}K \tag{1}$$

where $\mathrm{FACTV} = 4.72 \times 10^{-9}(104 - P'_{\mathrm{aO2(mean)}})^{4.9}$ for $P'_{\mathrm{aO2(mean)}} <$ 104 mm Hg and $\mathrm{FACTV} = 0$ for $P'_{\mathrm{aO2(mean)}} \geq 104$ mm Hg.

In this equation, AVR is the ratio of alveolar ventilation to the normal resting alveolar ventilation, $P'_{\mathrm{aCO2(mean)}}$ and $P'_{\mathrm{aO2(mean)}}$ represent the mean arterial partial pressures of carbon dioxide (CO_2) and oxygen (O_2) after transport delay from the heart to arterial receptors, respectively, and K is a constant.

Considering half of the ventilatory response to CO_2 and H^+ to be due to inputs from the arterial receptors and the other half resulting from the inputs from the central receptors [9], (1) can be re-written as

$$\begin{aligned}\mathrm{AVR} = {} & 0.11 \cdot H'^{+}_{a} + 0.131 \cdot P'_{a\mathrm{CO2(mean)}} + 0.11 \cdot H^+_C \\ & + 0.131 \cdot P_{\mathrm{CCO2}} + \mathrm{FACTV}\text{-}K\end{aligned} \tag{2}$$

where H'^{+}_{a} and H^+_C represent the hydrogen ion concentrations at the sites of the arterial and central receptors, respectively, and P_{CCO2} is the mean partial pressure of CO_2 at the site of the central receptors. According to [20], there is a linear relation between the hydrogen ion concentration and the partial pressure of CO_2 in the blood as

$$H'^{+}_{a} = 0.65.P'_{a\mathrm{CO2(mean)}} + 13.5 \tag{3}$$

and similarly for the CSF

$$H^+_{\mathrm{CSF}} = \left[\frac{\alpha.\beta}{(\mathrm{BHCO_3})_{\mathrm{CSF}}}\right] \cdot P_{\mathrm{CSFCO2}} \tag{4}$$

where H^+_{CSF}, P_{CSFCO2} and $(\mathrm{BHCO_3})_{\mathrm{CSF}}$ represent the hydrogen ion concentration, the partial pressure of CO_2 and bicarbonate concentration of the CSF, respectively, α is the solubility factor of CO_2 and β is carbonic acid dissociation constant in the CSF, respectively.

In COPD, the bicarbonate levels of the arterial blood and CSF are elevated to compensate for chronic hypercapnia [1, 5]. Incorporating the effects of bicarbonate levels increases in (3) and (4) yields:

$$H'^{+}_{a} = \frac{\left[0.65.P'_{\mathrm{aCO2(mean)}} + 13.5\right]}{\gamma} \tag{5}$$

$$H^+_{\mathrm{CSF}} = \left[\frac{\alpha.\beta}{(\mathrm{BHCO_3})_{\mathrm{CSF}}}\right] \cdot \frac{\mathrm{P_{CSFCO2}}}{\gamma} \tag{6}$$

where γ is a factor >1 (e.g. between 1.2 and 1.7) indicative of the rise in the bicarbonate level in the blood in COPD. Assuming the same relationship as (6) at the site of the central receptors

$$H^+_C = \left[\frac{\alpha.\beta}{(\mathrm{BHCO_3})_{\mathrm{CSF}}}\right] \frac{P_{\mathrm{CCO2}}}{\gamma} \tag{7}$$

Incorporating (5) and (7) in (2) yields

$$\begin{aligned}\mathrm{AVR} = {} & (0.0715) \cdot \frac{P'_{\mathrm{aCO2(mean)}}}{\gamma} + 0.11\left[\frac{\alpha.\beta}{(\mathrm{BHCO_3})_{\mathrm{CSF}}}\right] \cdot \frac{P_{\mathrm{CCO2}}}{\gamma} \\ & + 0.131 \cdot P'_{a\mathrm{CO2(mean)}} + 0.131 \cdot P_{\mathrm{CCO2}} \\ & + \mathrm{FACTV} + \frac{1.485}{\gamma} - K\end{aligned} \tag{8}$$

Substituting typical values of α, β, and $(\mathrm{BHCO_3})_{\mathrm{CSF}}$ as given in Appendix 2 in (8) results in

$$\begin{aligned}\mathrm{AVR} = {} & \left[0.131 + \frac{0.0715}{\gamma}\right] P'_{a\mathrm{CO2(mean)}} \\ & + \left[0.131 + \frac{0.10227}{\gamma}\right] \cdot P_{\mathrm{CCO2}} \\ & + \mathrm{FACTV} + \left[-K + \frac{1.485}{\gamma}\right]\end{aligned} \tag{9}$$

and $K = 18.885$.

In the system of the presented model, it is assumed that a neurogenic drive signal, MRV, which is the output of the metabolic unit, is provided to respiratory controller in exercise. Adding MRV to (9)

$$\begin{aligned}\mathrm{AVR} = {} & \left[0.131 + \frac{0.0715}{\gamma}\right] P'_{a\mathrm{CO2(mean)}} \\ & + \left[0.131 + \frac{0.10227}{\gamma}\right] P_{\mathrm{CCO2}} \\ & + \mathrm{FACTV} + \left[-K + \frac{1.485}{\gamma}\right] + \mathrm{MRV}\end{aligned} \tag{10}$$

where FACTV is defined as in (1).

Equation (10) has been used to simulate the 'ventilation controller' in COPD in Fig. 1. In using this equation, if AVR becomes negative or if $P'_{aCO2(mean)}$ <33 mm Hg, AVR becomes zero [9, 21].

'*The rate optimiser' and the breathing pattern*: The rate optimiser determines the optimal rate of breathing to minimise the respiratory work rate [19] based on the mechanical properties of the respiratory system [9]. By neglecting the forces related to inertia and turbulence in the lungs, a modified equation for the optimal breathing rate is used in the system [11]

$$f = \left[-\lambda.V_{\mathrm{D}} + \left(\lambda^2.V_{\mathrm{D}}^2 + 4.\lambda.\xi.\Pi^2.V_{\mathrm{D}}.V_{\mathrm{A}}^{\bullet}\right)^{0.5}\right]/\left(2.\Pi^2.\xi.V_{\mathrm{D}}\right) \quad (11)$$

where λ is respiratory system elastance, ξ is the airway resistance in the lungs, $V_{\mathrm{A}}^{\bullet}$ is alveolar ventilation, and V_{D} is the dead space volume found as

$$V_{\mathrm{D}} = K'.V_{\mathrm{DN}} \quad (12)$$

and V_{DN} is normal dead space found as [9]

$$V_{\mathrm{DN}} = 0.1698.V_{\mathrm{A}}^{\bullet} + 0.1587 \quad (13)$$

and K' is a factor >1 (e.g. 1.1–1.5) representing the effect of COPD on the dead space [7] as a result of the reduction in the ventilation/perfusion ratio [5].

Based on the outputs of the ventilation controller and the rate optimiser, the 'cyclic drive signal generator' in Fig. 1 generates a drive signal to the lungs that is updated for every breath. This generator can produce various signals such as a square wave, exponential and so on. If a sinusoidal signal that can be considered as the main harmonic of any cyclic signal is generated by this block, it will be given as

$$\frac{\mathrm{d}v}{\mathrm{d}t} = \Pi.V_{\mathrm{A}}^{\bullet}.\mathrm{Sin}\left(2.\Pi.f.t\right) \quad (14)$$

where v is the lung volume, and t is time. In the simulation studies presented in this paper, a sinusoidal signal is produced by the 'cyclic drive signal generator', according to (14). The external ventilation is found as

$$V_{\mathrm{E}} = V_{\mathrm{A}} + f1.V_{\mathrm{D}} \quad (15)$$

where V_{E} and V_{A} represent the external and alveolar ventilation, respectively (in l/min) and $f1$ is the breathing rate in breaths/min.

2.3. Control of blood flow: Cardiac output has been known to be a function of the metabolic rate [22], the arterial partial pressures of CO_2 [23] and O_2 [24], while the cerebral blood flow is known to be function of arterial tensions of CO_2 [25, 26], and O_2 [27, 28] but not the rate of metabolism. Detailed mathematical equations describing cardiac output and cerebral blood flow have been derived based on experimental data in the literature and used under static [29] and dynamic conditions [9]. Those equations are not given here because they are too long. In view of the fact that in general, COPD patients do not undergo high levels of exercise, for the purpose of this study, the mathematical descriptions for control of cardiac output and cerebral blood flow have been derived from experimental data as linear approximations up-to only moderate levels of exercise. The mathematical equations describing 'cardiac output controller' and 'cerebral blood flow controller' are described in the following sections.

2.3.1 Cardiac output controller: The cardiac output is described by a first-order dynamical equation as

$$\frac{\mathrm{d}Q}{\mathrm{d}t} = \frac{\left[Q_N + Q_M + Q_{\mathrm{CO}_2} + Q_{\mathrm{O}_2} - Q\right]}{\tau_3} \quad (16)$$

where Q is cardiac output, Q_N is cardiac output at rest, Q_M is the effect of exercise on cardiac output, Q_{O_2} and Q_{CO_2} are the effects of the arterial partial pressures of O_2 and CO_2 on cardiac output, respectively, and τ_3 is a time constant.

For Q_M, the following linear approximation equation was derived from data in moderate exercise in the literature [22]:

$$\begin{aligned} &Q_M = 0.36 \cdot (\mathrm{MRR} - 1) \cdot Q_N \text{ for MRR} > 1 \text{ and} \\ &Q_M = 0 \text{ for MRR} = 1 \end{aligned} \quad (17)$$

where MRR is the metabolic rate ratio (i.e. the ratio of the rate of metabolism to the basal rate).

A linear approximation equation in moderate exercise was derived for Q_{CO2} from the reported experimental data [23] as

$$\begin{aligned} &Q_{\mathrm{CO2}} = 0.054 \cdot \left(P_{a\mathrm{CO2}} - 42\right) \cdot Q_N \text{ for } P_{a\mathrm{CO2}} \geq 42 \text{ mmHg and} \\ &Q_{\mathrm{CO}_2} = 0 \text{ for } P_{a\mathrm{CO}_2} < 42 \text{ mmHg} \end{aligned} \quad (18)$$

where $P_{a\mathrm{CO2}}$ is the arterial partial pressure of CO_2.

For Q_{O_2}, the following linear approximation equation was derived from experimental data [24]:

$$\begin{aligned} &Q_{O2} = 0.008 \cdot \left(85 - P_{a\mathrm{O2}}\right) \cdot Q_N \text{ for } P_{a\mathrm{O2}} < 85 \text{ mmHg and} \\ &Q_{O2} = 0 \text{ for } P_{aO2} \geq 85 \text{ mm Hg} \end{aligned} \quad (19)$$

where $P_{a\mathrm{O2}}$ is the arterial partial pressure of O_2.

Equation sets (16)–(19) describe the cardiac output controller of the model. Q can be described as

$$Q = \mathrm{SV}x\mathrm{HR} \quad (20)$$

where SV is stroke volume and HR is heart rate. The SV is a function of the body posture and metabolic activity and is relatively constant at rest (e.g. 70 ml). This value increases by about 30–40% at the onset of activity and remains relatively constant during moderate exercise [30]. Approximate values of the HR can be found from the cardiac output produced by the model and (20), by using realistic approximate values for SV.

2.3.2 Cerebral blood flow controller: The blood flow to the brain does not change significantly in response to exercise but it is a function of $P_{a\mathrm{CO2}}$ [25, 26] and $P_{a\mathrm{O2}}$ [27, 28]. The following dynamical equation is used to describe the blood flow rate to the brain (Q_{B}) in the model:

$$\frac{\mathrm{d}Q_{\mathrm{B}}}{\mathrm{d}t} = \frac{\left[Q_{\mathrm{BN}} + Q_{\mathrm{BCO2}} + Q_{\mathrm{BO2}} - Q_{\mathrm{B}}\right]}{\tau_4} \quad (21)$$

where Q_{BN} is the normal brain blood flow rate, Q_{BCO2} and Q_{BO2} represent the effects of $P_{a\mathrm{CO2}}$ and $P_{a\mathrm{O2}}$ on the brain blood flow rate, respectively, and τ_4 is a time constant.

The following set of linear approximation formulas were derived for Q_{BCO2} in moderate exercise based on reported experimental data [25, 26]:

$$\begin{aligned} &Q_{\mathrm{BCO2}} = -0.015 \cdot Q_{\mathrm{BN}} \cdot \left(40 - P_{a\mathrm{CO2}}\right) \text{ for } P_{a\mathrm{CO2}} < 40 \text{ mmHg} \\ &Q_{\mathrm{BCO2}} = 0.1515.Q_{\mathrm{BN}} \cdot \left(P_{a\mathrm{CO2}} - 44\right) \text{ for } P_{a\mathrm{CO2}} \geq 44 \text{ mmHg} \\ &Q_{\mathrm{BCO2}} = 0 \text{ for } 40 \text{ mmHg} \leq P_{a\mathrm{CO2}} < 44 \text{ mmHg} \end{aligned} \quad (22)$$

For Q_{BO2}, a set of linear approximating formulas were derived in moderate exercise based on available data [27, 28]

$$Q_{BO2} = \left(0.562\text{-}0.006P_{aO2}\right) \cdot Q_{BN} \text{ for } P_{aO2} < 87 \text{ mmHg}$$
$$Q_{BO2} = 0 \text{ for } P_{aO2} \geq 87 \text{ mmHg} \quad (23)$$

Equation sets (21)–(23) describe the cerebral blood flow controller of the model.

The blood flow rate in the body tissues, Q_T (excluding the brain) is found as

$$Q_T = Q - Q_B \quad (24)$$

3. Example results: The mathematical model was tested at rest and moderate exercise with and without oxygen supplementation at two different stages of COPD. In the more advanced stage of the disease, exercise simulations were not done without oxygen supplementation. Table 1 shows the steady-state values of several selected variables of the model under different test conditions.

In the simulation results of Table 1, the steady-state values at rest were obtained after 50 min of simulation and in exercise after 20 min. The respiratory elastance was 28 cm H_2O/l, and airway resistance was 10 cm H_2O/l/s. Two stages of COPD are considered. Stage 1 represents a moderate level of the disease while stage 2 represents a more advanced level of the illness. The factor γ in the ventilation controller that indicates the extent of acid–base shifting in COPD is 1.3 in COPD stage 1 and is 1.5 in COPD stage 2.

Table 1 Steady-state results of the model at rest and in moderate exercise in COPD

TEST COND.			SIMU. RES.					
F_{IO2}	Stg.	MRR	P'_{aO2}	P'_{aCO2}	$f1$	V_E	Q	Q_B
Resting								
0.21	1	1	65.4	45.5	9.9	5.15	6.47	0.9
0.21	2	1	62.1	47.8	10.6	5.75	7.41	1.21
0.35	1	1	165.6	45.75	11.5	6.29	5.9	0.9
0.35	2	1	161.4	49.1	9.5	5	6.73	1.25
Mod. Exer.								
0.21	1	3	60	44.8	18.8	12.87	15.1	0.85
0.35	1	3	157.6	45.7	18.5	12.61	9.14	0.81
0.35	2	3	158.7	48.2	18.4	12.43	9.8	1.03

P'_{aO2} and P'_{aCO2} are in mm Hg, $f1$ is in breaths/min, V_E, as well as Q, and Q_B are given in lit/min.

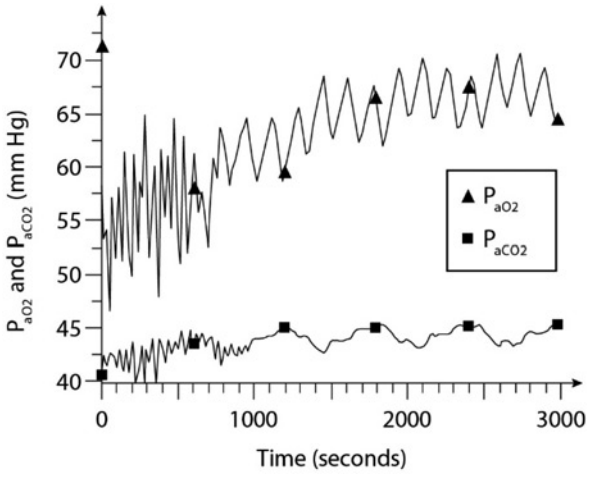

Fig. 2 *Example simulation results at rest in stage 1, COPD, with no oxygen supplementation*

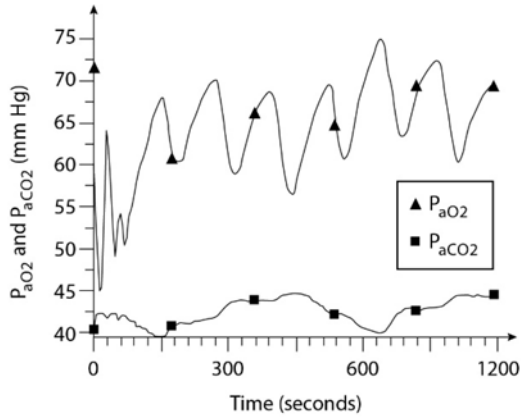

Fig. 3 *Example simulation results in moderate exercise in COPD, stage 1, with no oxygen supplementation*

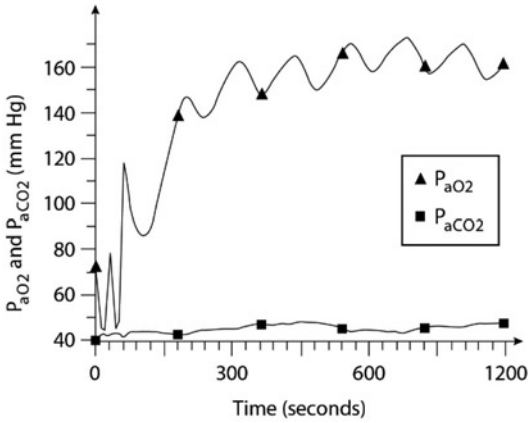

Fig. 4 *Example simulation results in moderate exercise in stage 2, COPD, with oxygen supplementation ($F_{IO2} = 0.35$)*

Figs. 2–4 show examples of the dynamical responses of the model. Fig. 2 shows the P'_{aO2} and P'_{aCO2} responses of the model in moderate COPD (stage 1) at rest with no oxygen supplementation. As is seen, P'_{aO2} stabilises around 65 mm Hg in about 30 min and P'_{aCO2} is around 45 mm Hg indicative of hypoxemia and hypercapnia.

Fig. 3 shows the exercise simulation results of the model in moderate COPD when MRR = 3 and without oxygen supplementation. As is seen, P'_{aO2} goes up to about 70 mm Hg in about 9 min and P'_{aCO2} is about 43–45 mm Hg.

Fig. 4 shows the dynamic simulation results of P'_{aO2} and P'_{aCO2} in moderate exercise (MRR = 3) for a patient with stage 2 COPD while oxygen supplementation ($F_{IO2} = 0.35$) is applied. As can be seen, P'_{aO2} responds to oxygen supplementation while P'_{aCO2} approaches to about 50 mm Hg due to CO_2 retention in about 7.5 min.

4. Discussion: As can be seen from the simulation results of Table 1, hypoxemia and hypercapnia are observed at rest in patients breathing room air ($F_{IO2} = 0.21$), at moderate COPD (i.e. stage 1) and in more advanced stage of the disease (i.e. stage 2). It can be seen that hypoxemia and hypercapnia are worsened at rest in patients with more advanced COPD. The P'_{aO2} level changes from 65.4 to 62.1 mm Hg and P'_{aCO2} increases from 45.5 to 47.8 mm Hg as COPD advances to a higher stage. When oxygen supplementation is used at rest ($F_{IO2} = 0.35$), P'_{aO2} rises, but P'_{aCO2} also increases causing more hypercapnia. In moderate COPD, P'_{aCO2} slightly increases to 45.75 mm Hg with oxygen supplementation at rest, while in more advanced COPD, P'_{aCO2} increases to 49.1 mm Hg showing more highly pronounced

hypercapnia with oxygen supplementation. This is known as CO_2 retention in response to oxygen supplementation in COPD patients. These results are in general agreement with clinical observations [31, 32].

In moderate exercise (MRR = 3), unlike normal subjects whose blood gases are not affected by exercise, hypoxemia and hypercapnia are observed in COPD patients. When oxygen supplementation is used in exercise ($F_{IO2} = 0.35$), P'_{aO2} rises, but P'_{aCO2} also increases and the increase in P'_{aCO2} is higher in the more advanced stage of the disease to 48.2 mm Hg. The results of the model in moderate exercise are seen to be in general agreement with experimental data [32–34].

The dynamic simulation results of Figs. 2–4 show the effects of COPD on the blood gases at rest and in moderate exercise with and without oxygen supplementation. These results show the persistence of hypercapnia at two stages of COPD and the effects of CO_2 retention with oxygen supplementation that are exacerbated at the higher stage of the disease. These results are seen to be in general agreement with experimental data [31, 32, 34].

5. Conclusion: In summary, it is known that in COPD the ventilation/perfusion ratio is adversely affected due to damages to the alveoli [5]. At the same time, the inflammation in the bronchi causes the respiratory airway resistance to increase [1]. The combination of these factors causes significant increase in the work of breathing to maintain adequate ventilation and regulate blood gases in the normal range. As a consequence, the level of effective ventilation decreases in COPD over time which causes hypoxemia and hypercapnia [31, 35]. These effects in turn cause the bicarbonate concentration of the blood and the CSF to rise above normal to keep the blood pH level within an acceptable range [1]. This chronic acid–base adjustment reduces the effect of CO_2 as a stimulus to ventilation. In the model presented in this study, the ventilation controller includes the effects of chronic acid–base shifting in COPD. This model includes a cyclical changing lung volume, a discrete and detailed controller and a plant that includes the body tissue, the brain tissue, a CSF compartment, central and peripheral receptors, cardiac output and cerebral blood flow controllers and a metabolism mechanism that produces a neurogenic stimulus to ventilation in exercise. The simulation results of this model are seen to be in general agreement with the reported experimental observations.

More detailed simulation experiments under various conditions in the future may enhance the applications of the model as well as the understanding of different mechanisms at work at different stages of COPD. Future work may also include consideration of chronic changes in the respiratory muscle physiology under COPD.

6 References

[1] Bruno C.M., Valenti M.: 'Acid-base disorders in patients with chronic obstructive pulmonary disease: a pathophysiological review', *J. Biomed. Biotech.*, 2012, **2012**, article ID 915150, pp. 1–8

[2] O'Donnell D.E., Parker C.M.: 'COPD exacerbations. 3: pathophysiology', *Thorax*, 2006, **61**, pp. 354–361

[3] Colac Y., Afzal S., Nordestgaard B.G., *ET AL.*: 'Prevalence, characteristics, and prognosis of early chronic obstructive pulmonary disease', *Am. J. Resp. Crit. Care Med.*, 2020, **201**, pp. 671–680

[4] Biselli P., Fricke K., Grote L, *ET AL.*: 'Reductions in dead space ventilation with nasal high flow depend on physiological dead space volume: metabolic hood measurements during sleep in patients with COPD and controls', *Eur. Respir. J.*, 2018, **51**, pp. 1–9

[5] Jacono F.J.: 'Control of ventilation in COPD and lung injury', *Respir. Physiol. Neurobiol.*, 2013, **189**, pp. 371–376

[6] Sinha P., Flower O., Soni N.: 'Deadspace ventilation: a waste of breath!', *Intensive Care Med.*, 2011, **37**, pp. 735–746

[7] Farah R., Makhoul N.: 'Can dead space fraction predict the length of mechanical ventilation in exacerbated COPD patients?', *Int. J. COPD*, 2009, **4**, pp. 437–441

[8] Grodins F.S., Buell J., Bart A.J.: 'Mathematical analysis and digital simulation of the respiratory control system', *J. Appl. Physiol.*, 1967, **22**, pp. 260–275

[9] Fincham W.F., Tehrani F.T.: 'A mathematical model of the human respiratory system', *J. Biomed. Eng.*, 1983, **5**, pp. 125–133

[10] Revow M., England S.J., O'Beirne H., Bryan A.C.: 'A model of the maturation of respiratory control in the Newborn infant', *IEEE Trans. Biomed. Eng.*, 1989, **36**, pp. 414–423

[11] Tehrani F.T.: 'Mathematical analysis and computer simulation of the respiratory system in the newborn infant', *IEEE Trans. Biomed. Eng.*, 1993, **40**, pp. 475–481

[12] Hernandez A.M., Mananas M.A., Costa-Castello R.: 'Learning respiratory system functions in BME studies by means of a virtual laboratory: Respilab', *IEEE Trans. Edu.*, 2008, **51**, pp. 24–34

[13] Serna L.Y., Mananas M.A., Hernandez A.M., Rabinovich R.A.: 'An improved dynamic model for the respiratory response to exercise', *Front. Physiol.*, 2018, **9**, article 69, pp. 1–16

[14] Wang W., Das A., Ali T., Cole O., Chikhani M., Haque M., Hardman J.G., Bates D.G.: 'Can computer simulators accurately represent the pathophysiology of individual COPD patients?', *Intensive Care Med. Exp.*, 2014, **2**, pp. 1–14

[15] Loeppky J.A., Caprihan A., Altobelli S.A., Icenogle M.V., Scotto P., Vidal, Melo M.F.: 'Validation of a two-compartment model of ventilation/ perfusion distribution', *Respir. Physiol. Neurobiol.*, 2006, **151**, pp. 74–92

[16] Parkes M.J.: 'Evaluating the importance of the carotid chemoreceptors in controlling breathing during exercise in man', *Biomed. Res. Int.*, 2013, **2013**, article ID. 893506, pp. 1–18

[17] Moreira T.S., Takakura A.C., Damasceno R.S., Falquetto B., Totola L.T., Sobrinho C.R., Ragioto D.T., Zolezi F.P.: 'Central chemoreceptors and neural mechanisms of cardiorespiratory control', *Braz. J. Med. Biol. Res.*, 2011, **44**, pp. 883–889

[18] Richter D.W., Smith J.C.: 'Respiratory rhythm generation in vivo', *Phsiology*, 2014, **29**, pp. 58–71

[19] Otis A.B., Fenn W.O., Rahn H.: 'Mechanics of breathing in man', *J. Appl. Physiol.*, 1950, **2**, pp. 592–607

[20] Gray J.S.: 'Pulmonary Ventilation and its Physiological Regulation' (Charles C. Thomas, Chicago, IL, 1949)

[21] Nielsen M., Smith H.: 'Studies on the regulation of respiration in acute hypoxia', *Acta Physiol. Scand.*, 1952, **24**, pp. 293–313

[22] Ruch T.C., Patton H.D. (Eds.): 'Physiology and Biophysics' (W. B. Saunders, Philadelphia, PA, 1966, 19th edn.), p. 658

[23] Richardson D.W., Wasserman A.J., Patterson J.L.Jr: 'General and regional circulatory responses to change in blood pH and carbon dioxide tension', *J. Clin. Invest.*, 1961, **40**, pp. 31–43

[24] Scarborough W.R, Penneys R., Thomas C.B., Baker B.M.Jr, Mason R.E.: 'The cardiovascular effect of induced controlled anoxemia', *Circulation*, 1951, **4**, pp. 190–210

[25] Wasserman A.J., Patterson J.L.Jr: 'The cerebral vascular response to reduction in arterial carbon dioxide tension', *J. Clin. Invest.*, 1961, **40**, pp. 1297–1303

[26] Patterson J.L.Jr, Heyman A., Battey L.L., *ET AL.*: 'Threshold response of the cerebral vessels of man to increase in blood carbon dioxide', *J. Clin. Invest.*, 1955, **34**, pp. 1857–1864

[27] Shimojyo S., Scheinberg P., Kogure K., Reinmuth O.M.: 'The effects of graded hypoxia upon transient cerebral blood flow and oxygen consumption', *Neurology*, 1968, **18**, pp. 127–133

[28] Shapiro W., Wasserman A.J., Baker J.P., Patterson J.L.Jr: 'Cerebrovascular response to acute hypocapnic and eucapnic hypoxia in normal man', *J. Clin. Invest.*, 1970, **49**, pp. 2362–2368

[29] Fincham W., Tehrani F.T.: 'On the regulation of cardiac output and cerebral blood flow', *J. Biomed. Eng.*, 1983, **5**, pp. 73–75

[30] Higginbotham M.B., Morris K.G., Williams R.S., McHale P.A., Coleman R.E., Cobb F.R.: 'Regulation of stroke volume during submaximal and maximal upright exercise in normal man', *Circ. Res.*, 1986, **58**, pp. 281–291

[31] Yu L.H., Wu Y.C.: 'Clinical significance of coagulation function combined with blood gas analysis and serum NT-proBNP detection in COPD patients', *J. Hainan Medical University*, 2017, **23**, pp. 48–51

[32] O'Donnell D.E., D'Arsigny C., Fitzpatrick M., Webb K.A.: 'Exercise hypercapnia in advanced chronic obstructive pulmonary Disease', *Am. J. Respir. Crit. Care Med.*, 2002, **166**, pp. 663–668

[33] Christensen C.C., Ryg M.S., Edvardsen A, Skjonsberg O.H.: 'Effect of exercise mode on oxygen uptake and blood gases in COPD patients', *Respir. Med.*, 2004, **98**, pp. 656–660

[34] Casciari R.J., Fairshter R.D., Harrison A., Morrison J.T., Blackburn C., Wilson A.F.: 'Effects of breathing retraining in patients with

chronic obstructive pulmonary disease', *Chest*, 1981, **79**, pp. 393–398
[35] Halim A.A., Adawy Z., Sayed M.: 'Role of neopterin among COPD patients', *Egyp. J. Chest Dis. Tubercul.*, 2016, **65**, pp. 23–27

7. Appendix 1

Additional equations:

Lungs:

For CO_2:

$$\left(C_{\mathrm{VTCO2}}\text{-}C_{a\mathrm{CO2}}\right)Q_T + \left(C_{\mathrm{VBCO2}} - C_{a\mathrm{CO2}}\right)Q_B = \left[\frac{v}{\left(P_b - 47\right)}\right]\frac{\mathrm{dP_{ACO2}}}{\mathrm{d}t} + \mathrm{FACT1} \tag{25}$$

For O_2:

$$\left(C_{a\mathrm{O2}} - C_{\mathrm{VTO2}}\right)Q_{\mathrm{T}} + \left(C_{a\mathrm{O2}}\text{-}C_{\mathrm{VBO2}}\right)Q_{\mathrm{B}} = \left[\frac{-v}{\left(P_b - 47\right)}\right]\frac{\mathrm{d}P_{\mathrm{AO2}}}{\mathrm{d}t} + \mathrm{FACT2} \tag{26}$$

where in inspiration that $\mathrm{d}v/\mathrm{d}t \geq 0$:

$$\mathrm{FACT1} = \left[\frac{\left(P_{\mathrm{ACO2}}\text{-}P_{\mathrm{ICO2}}\right)}{\left(P_b - 47\right)}\right]\frac{\mathrm{d}v}{\mathrm{d}t}$$

$$\mathrm{FACT2} = \left[\frac{\left(P_{\mathrm{IO2}} - P_{\mathrm{AO2}}\right)}{\left(P_b - 47\right)}\right]\frac{\mathrm{d}v}{\mathrm{d}t}$$

and during expiration that $\mathrm{d}v/\mathrm{d}t < 0$: FACT1 = FACT2 = 0.

Body tissue:

$$C_{\mathrm{VTCO2}}.Q_{\mathrm{T}} = C_{a\mathrm{CO2}}.Q_{\mathrm{T}} + MR_{\mathrm{TCO2}}\text{-}S_{\mathrm{T}}.\ \frac{\mathrm{dC_{VTCO2}}}{\mathrm{d}t} \tag{27}$$

$$C_{\mathrm{VTO2}}.Q_{\mathrm{T}} = C_{a\mathrm{O2}}.Q_{\mathrm{T}} - MR_{\mathrm{TO2}}\text{-}S_{\mathrm{T}}\ \frac{\mathrm{d}C_{\mathrm{VTO2}}}{\mathrm{d}t} \tag{28}$$

Arterial transport delay:

$$C'_{a\mathrm{CO2}} = C_{a\mathrm{CO2}}(t - T) \tag{29}$$

$$C'_{a\mathrm{O2}} = C_{a\mathrm{O2}}(t - T) \tag{30}$$

$$P'_{a\mathrm{CO2}} = P_{a\mathrm{CO2}}(t - T) \tag{31}$$

$$P'_{a\mathrm{CO2}} = P_{a\mathrm{O2}}(t - T) \tag{32}$$

Brain tissue:

$$C_{\mathrm{VBCO2}}.Q_{\mathrm{B}} = C'_{a\mathrm{CO2}}.Q_{\mathrm{B}} + \mathrm{MR_{BCO2}}\text{-}S_{\mathrm{B}}.\ \frac{\mathrm{dC_{VBCO2}}}{\mathrm{d}t} \tag{33}$$

$$C_{\mathrm{VBO2}}.Q_{\mathrm{B}} = C'_{a\mathrm{O2}}.Q_{\mathrm{B}}\text{-}MR_{\mathrm{BO2}}\text{-}S_{\mathrm{B}}.\ \frac{\mathrm{dC_{VBO2}}}{\mathrm{d}t} \tag{34}$$

The CSF compartment:

$$\frac{\mathrm{dP_{CSFCO2}}}{\mathrm{d}t}.K_5 = \left[P_{\mathrm{VBCO2}}\text{-}P_{\mathrm{CSFCO2}}\right] \tag{35}$$

Central receptor equation:

$$P_{\mathrm{CCO2}} = P_{\mathrm{VBCO2}} + \left[P_{\mathrm{CSFCO2}}\text{-}P_{\mathrm{VBCO2}}\right].\exp\left[-d.\left[Q_{\mathrm{B}}.K_4\right]^{0.5}\right] \tag{36}$$

The metabolic unit:

$$\frac{\mathrm{dMR_{TO2}}}{\mathrm{d}t}.\tau_1 = \left[\mathrm{MIF\text{-}MR_{TO2}}\right] \tag{37}$$

$$\mathrm{MR_{TCO2}} = 0.81534.\mathrm{MR_{TO2}} \tag{38}$$

$$\mathrm{MR_{O2}} = \mathrm{MR_{TO2}} + \mathrm{MR_{BO2}} \tag{39}$$

$$\mathrm{MR_{CO2}} = \mathrm{MR}_{TCO2} + \mathrm{MR}_{BCO2} \tag{40}$$

$$\mathrm{MRR} = \frac{\mathrm{MR_{O2}}}{\mathrm{MR_{O2}(basal)}} \tag{41}$$

$$\frac{\mathrm{dMRV}}{\mathrm{d}t}\cdot\tau_2 = [\mathrm{MRR} - 1] - \mathrm{MRV} \tag{42}$$

Blood gas relationships:

$$C_{\mathrm{O2}} = K_1.\left[1 - \mathrm{e}^{(-K_{2.}\ P_{\mathrm{O2}})}\right]^2 \tag{43}$$

$$C_{\mathrm{CO2}} = K_3.P_{\mathrm{CO2}} \tag{44}$$

8. Appendix 2

Glossary of symbols is given in Table 2. The main symbols specify the parameters or variables and the subscripts denote a chemical or a location of the parameter/variable in the model. $\bar{X}$ denotes the mean value of X and X' denotes the time-delayed value of X.

Table 2 Glossary of symbols

Symbol	Definition	Value/unit (where applicable)
AVR	alveolar ventilation ratio	
$BHCO_3$	bicarbonate concentration	0.58 l(STPD)/l
C	volume concentration of gas in the blood	l(STPD)/l
d	depth of central receptor below the surface of the medulla	15×10^{-3} cm
F	breathing frequency	breaths/s
fl	breathing frequency	breaths/min
F	fractional composition of gas	
FACTN	factor n as specified in text	
H^+	hydrogen ion concentration	nmoles/l
K	ventilation controller constant	
K'	dead space COPD factor	
K_1	blood gas dissociation constant for oxygen	0.2
K_2	blood gas dissociation constant for oxygen	0.046 [mm Hg]$^{-1}$
K_3	blood gas dissociation constant for carbon dioxide	0.016 [mm Hg]$^{-1}$
K_4	central receptor constant	346×10^3 s. cm^{-2}.l^{-1}
K_5	carbon dioxide diffusion time constant	320 s
MIF	metabolic input function to tissue	l/s
MR	metabolic rate	l/s
MR_B	metabolic rate in brain	basal rate for oxygen: 0.000925 l/s basal rate for carbon dioxide: 0.0009 l/s
MR_T	metabolic rate in body tissue	basal rate for oxygen: 0.00352 l/s basal rate for carbon dioxide: 0.00287 l/s

Continued

TABLE 2 *Continued*

Symbol	Definition	Value/unit (where applicable)
MRR	metabolic rate ratio (ratio of actual metabolic rate to basal metabolic rate)	
MRV	neurogenic metabolic drive to ventilation	
P	partial pressure or gas pressure	mm Hg
Q	blood flow rate	l/s
Q_T	blood flow rate in body tissue	basal rate: 0.07083 l/s
Q_B	blood flow rate in brain	basal rate: 0.0125 l/s
S	equivalent gas storage space	l
S_T	equivalent gas storage space in body tissue	13 l
S_B	equivalent gas storage space in brain	1.1 l
T	arterial blood transport delay	10 s
T	time	s
V	volume	l
$V_A^\bullet$	effective alveolar ventilation	l/s. Normal value at rest: 0.0673 l/s
V_A	effective alveolar ventilation	l/min
V_D	dead space	l
V_E	external ventilation	l/min
v	volume of the lungs	l
τ_1	exercise dynamic factor	30 s
τ_2	neural metabolic drive dynamic factor	50 s
τ_3	cardiac output dynamic factor	3 s
τ_4	cerebral blood flow dynamic factor	3 s
α	solubility factor for carbon dioxide in CSF	6.783×10^{-4} l (STPD)/l/mm Hg
β	carbonic acid dissociation constant in CSF	795 nmoles/l
γ	acid–base adjustment factor for bicarbonate concentration in COPD	
λ	respiratory system elastance	cm H_2O/l
ξ	respiratory airway resistance	cm H_2O/l(BTPS)/s

Subscripts	
a	arterial blood
A	alveolar gas
b	barometric condition
B	brain
C	a point in the neighbourhood of central receptors
CO_2	carbon dioxide
CSF	CSF
D	dead space
E	external ventilation
I	inspired gas
M	metabolic
N	normal
O_2	oxygen
T	body tissue (excluding brain)
V	venous blood
VB	brain venous blood
VT	tissue venous blood